Report of LACE stay at ZAMG in Vienna
20.04.2015-22.05.2015

PARAMETERIZATION OF OROGRAPHIC EFFECTS ON SURFACE RADIATION IN AROME

Supervisor:
Christoph Wittmann
christoph.wittmann@zamg.ac.at

Consultant:
Clemens Wastl
clemens.wastl@zamg.ac.at

Author:
Martin Dian
martin.dian@shmu.sk

Contents

1. Introduction

It is well known that the radiation balance is affected by terrain orography. The amount of downwelling shortwave radiation SWR depends on the local slope and aspect angle.[1] The balance of longwave radiation LWR is affected by the sky view restriction.[2] Without this requirements are gridpoints assumed as flat and effectively homogeneous. Orographic effects becomes increasingly important, when we require for example forecasts for two close places which one is situated on the bottom of deep valley and the other on the top of the mountain. Because the resolution of models is a few kilometers, thus these effects on the grid scale are minimal.

Müller and Sherer proposed high-resolution subgrid-scale scheme using the digital elevation model thats the resolution can be$\lesssim 100 \times 100$ meters.[3] They parametrized SWR effects due to the different slope angle and direction, relief shadows (SWR) and restricted the sky view for both SWR and LWR.

2. Orographic parametrization

In this section we present the new orographic radiation parametrization, that was used in HIRLAM. We follow the approach according Müller et al. and Senkova et al, see Ref. [3, 4].

2.1 Short-wave solar radiation

The downwelling solar radiation on the flat place without the surrounding mountains consist of the sum of the direct solar radiation prependicular to the solar beam $S_{\downarrow 0,dir}$ and the diffuse $S_{\downarrow 0,diff}$ solar radiation:

$$S_{\downarrow 0} = S_{\downarrow 0,dir} \sin(h_s) + S_{\downarrow 0,diff}, \tag{2.1}$$

where h_s is height of the Sun. Subscripts 0 marks the radiation fluxes on the flat places. As we can see on the figure 2.1, the direct solar radiation is scattered by atmosphere, aerosols and clouds, reflected by clouds and slopes of mountains. Obstacles, like mountains, trees etc. decrease the solar radiation due to shadowing.

Slope parameter:

According to Kondratyev el al. [5] the direct solar flux $S_{\downarrow,dir}$ at the slope depends on the direct solar flux on the flat surface $S_{\downarrow 0,dir}$ as:

$$S_{\downarrow,dir} = S_{\downarrow 0,dir} \cos(n), \tag{2.2}$$

where n is an angle beetween normal of the surface and the solar beam, see fig 2.2

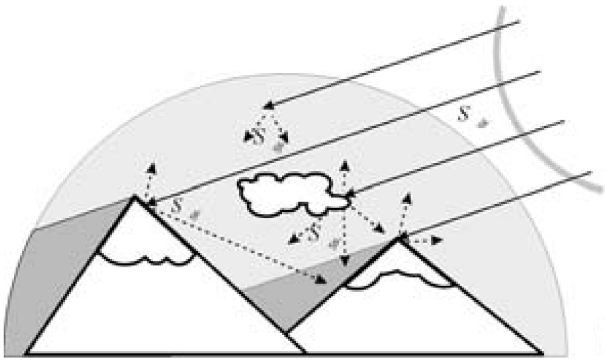

Figure 2.1: SWR fluxes over mountainous terrain.[4]

and

$$\cos(n) = \cos(h_m)\sin(h_s) + \sin(h_m)\cos(h_s)\cos(a_s - a_m), \tag{2.3}$$

where h_m is angle of the slope, h_s is height of the Sun above horizon, a_m is the aspect angle of the slope and a_s is the solar azimuth. Both of a_m and a_s are defined clockwise from the north. Both of a_s and h_s depend on the time and location according to the standard astronomical formulaes.

Due to the larger area at the real slope in the gridpoints which are considered in the model as a flat area, the average gridpoint direct solar flux is multiplied by $1/\cos(h_m)$:

$$S_{\downarrow,dir,grid} = \frac{S_{\downarrow,dir}}{\cos(h_m)}. \tag{2.4}$$

Plugging (2.2) and (2.3) into (2.4) we get:

$$S_{\downarrow,dir,grid} = \delta_{sl}(t) S_{\downarrow 0,dir}, \tag{2.5}$$

where we have introduced the time dependent parameter $\delta_{sl}(t)$:[1]

$$\delta_{sl}(t) = \sin(h_s)\left[1 + \frac{\tan(h_m)}{\tan(h_s)}\cos(a_s - a_m)\right]. \tag{2.6}$$

Shadow factor:

When the sun is below local horizon, there is no direct solar radiation. Let us denote the local orographic horizon as $h_h(\theta)$, where θ is azimuth, again defined clockwise from the north. We define the next time dependent parameter: shadow fraction $\delta_{sh}(h_s(t), a_s(t))$ which is defined:

$$\delta_{sh}(h_s(t), a_s(t)) = \begin{cases} 1 & h_s(t) > h_h(a_s(t)) \\ 0 & h_s(t) < h_h(a_s(t)). \end{cases} \tag{2.7}$$

The direct solar radiation is now given by:

$$S_{\downarrow,dir,grid,sh} = \delta_{sh}(t) S_{\downarrow,dir,grid} = \delta_{sh}(t)\delta_{sl}(t) S_{\downarrow 0,dir}. \tag{2.8}$$

[1]It should be noted that for $h_m = 0$ holds: $\delta_{sl}(t) = \sin(h_s)$ so $S_{\downarrow,dir,grid} = \sin(h_s) S_{\downarrow 0,dir}$, that was expected.

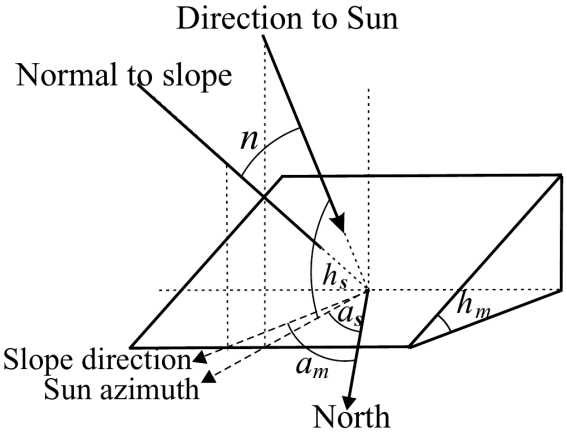

Figure 2.2: SWR fluxes over mountainous terrain.[4]

Sky view factor:

The diffuse solar radiation is restricted by the local horizon. The total area of visible sky normalized to 1 is given by:

$$\delta_{sv} = 1 - \frac{1}{2\pi}\int_0^{2\pi} \sin[h_h(\theta)]d\theta, \tag{2.9}$$

where $h_h(\theta)$ is a local horizon angle. From now we call δ_{sv} as a sky view factor (SVF). So the diffuse radiation $S_{\downarrow,diff,grid,sv}$ can be expressed as:

$$S_{\downarrow,diff,grid,sv} = \delta_{sv}\frac{S_{\downarrow 0,diff}}{\cos(h_m)} + \alpha(1-\delta_{sv})S_{\downarrow,surf}, \tag{2.10}$$

where α is the surface albedo of the mountains and $S_{\downarrow,surf}$ is the global radiation over the surrounding surface. The factor $\frac{1}{\cos(h_m)}$ in the first term is again due to larger grid area. For our purpose we do the next approximation:

$$S_{\downarrow,surf} \approx \sin(h_s)S_{\downarrow 0,dir} + S_{\downarrow 0,diff}. \tag{2.11}$$

Now we can write totally:

$$S_{\downarrow,grid} = S_{\downarrow,dir,grid,sh} + S_{\downarrow,diff,grid,sv}, \tag{2.12}$$

plugging sequentially (2.5), (2.8), (2.10) and(2.11) into (2.12) we get:

$$S_{\downarrow,grid} = S_{\downarrow 0,dir}(\delta_{sh}(t)\delta_{sl}(t) + \alpha(1-\delta_{sv})\sin(h_s)) + S_{\downarrow 0,diff}\left[\frac{\delta_{sv}}{\cos(h_m)} + \alpha(1-\delta_{sv})\right]. \tag{2.13}$$

In the flat place without mountains where $\delta_{sh} = 1, \delta_{sl} = \sin(h_s), \delta_{sv} = 1, \cos(h_m) = 1$ the total SWR is:

$$S_{\downarrow,grid} = S_{\downarrow 0,dir}\sin(h_s) + S_{\downarrow 0,diff}, \tag{2.14}$$

that is the same relation as in (2.1) as was expected.

Finally we approximate the upwelling shortwave flux as:

$$S_{\uparrow} \approx \alpha S_{\downarrow,0} \tag{2.15}$$

2.2 Long-wave radiation

The downwelling long-wave radiation (LWR) $F_{\downarrow}$ consist of the radiation emitted from the sky and clouds. In the mountain area is LWR restricted by the sky view, but amplified by the sourunding slopes, see 2.3:

$$F_{\downarrow} = \delta_{sv} F_{\downarrow 0} + \epsilon \sigma T^4 (1 - \delta_{sv}), \tag{2.16}$$

where $F_{\downarrow 0}$ is LWR from the sky and clouds without mountains, ϵ is emissivity of terain, σ is Stefan–Boltzmann constant and T is temperature of sourunding slopes. The upwelling long-wave radiation is approx:

$$F_{\uparrow} = \delta_{sv} F_{\uparrow 0} + \epsilon \sigma T^4 (1 - \delta_{sv}), \tag{2.17}$$

where $F_{\uparrow 0}$ is upwelling LWR from the terrain without mountains. The net LWR flux is than:

$$F_{net} = F_{\downarrow} - F_{\uparrow} = \delta_{sv} F_{net,0}, \tag{2.18}$$

where

$$F_{net,0} = F_{\downarrow 0} - F_{\downarrow 0} \tag{2.19}$$

and $F_{net,0}$ is the net long-wave flux without mountains. We can see from (2.18) thus the long-wave cooling during the nights is smaller in the deep valleys where is sky view small and larger at the mountain tops.

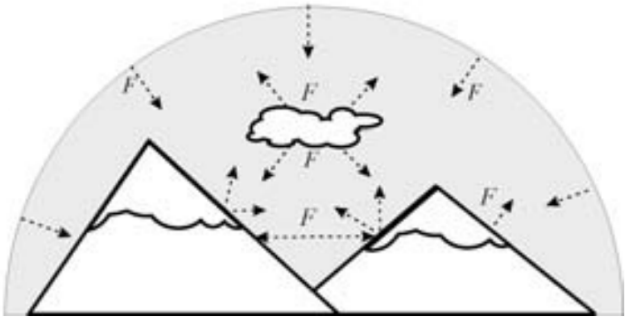

Figure 2.3: LWR fluxes over mountainous terrain.[4]

3. Orographic factors

Because the resolution of digital elevation model on the subgrid space can be $\lesssim 100 \times 100$ meters there is a problem with huge amount of subgrid values of slopes, shadows and sky view factors. In work [3] and [4] was introduced the simpification which store only important information of the orography in grid points in a 34 time independent numbers for each grid points.

Slope angles and fraction aspects:

The slope parameter is time dependent (solar height and azimuth) and dependent on its location. Due to complications with a huge amount subgrid time depend values it was done some simpification of (2.6).[4] It was introduced 8 directions oriented to N,NE,E,SE,S,SW,W and NW. They correspond to the 8 values of model azimuth parameters $a_{m,1}..a_{m,8}$. The equation (2.6) for the slope parameter can be now rewritten as:

$$\boxed{\delta_{sl}(t) = \sin(h_s(t)) + \cos(h_s(t)) \sum_{i=1}^{8} f_i \tan(h_m, i) \cos(a_s(t) - a_{m,i}),} \tag{3.1}$$

where f_i is ratio of slopes in the subgrids oriented in the direction centered to $a_{m,i}$ and $h_{m,i}$ is the mean value of slope angle. So for each grid point it is stored for the slope parameter only 8 values of f_i and 8 values of $h_{m,i}$.

For the sake of completeness it is stored also the average slope angles h in the grid points.

Local horizon angles:

The local horizon angle in eq. (2.9) for the sky view restriction is calculated only for 8 directions $h_{h,1}..h_{h,8}$, due to same reasons as for the slope angles. The orientations of the local horizon angles are also same. For each $h_{h,i}$ is calculated totally 45 one-degre local horizon angles, where the result $h_{h,i}$ is an arithmetical average of the all one-degre subdirections:

$$h_{h,i} = \frac{1}{45} \sum_{j=1}^{45} h_{h,i_j}, \tag{3.2}$$

where h_{h,i_j} are the local horizons in the diretions i_j, where :

$$h_{h,i_j} = \max_{0<\Delta<\Delta_{max}} \left[\arctan \frac{e_o(\Delta) - e_v(0)}{\Delta} \right], \tag{3.3}$$

$e_o(\Delta)$ is the elevation of the obstacle at the distance Δ, $e_v(0)$ is the elavation of the viewing point and Δ_{max} is the max. distance which is considered.

Finally, the equation (2.9) for the sky view factor can be rewritten in discreate form:[1]

$$\boxed{\delta_{sv} = 1 - \frac{1}{8}\sum_{i=1}^{8} \sin(h_{h,i}).} \tag{3.4}$$

Shadow coefficients:

According to the (2.7) shadow factor depends on the height of the Sun h_s. For the calculation of shadow factor we find also the minimum and maximum value of 1° subdirections in the sectors i:

$$h_{h,i,min} = \min_j h_{h,i_j}, \qquad h_{h,i,max} = \max_j h_{h,i_j}. \tag{3.5}$$

Between these values we assume the linear relationship for the shadow fraction:

$$\boxed{\delta_{sh,i}(t) = A_i \sin(h_s(t)) + B_i,} \tag{3.6}$$

where coefficients A_i and B_i are determined from the following conditions:

$$\begin{array}{l} \delta_{sh,i} = 0 \quad \text{if } \mathrm{h_s} = \mathrm{h_{h,i,min}} \\ \delta_{sh,i} = 1 \quad \text{if } \mathrm{h_s} = \mathrm{h_{h,i,max}}. \end{array} \tag{3.7}$$

So totally the output PGD file comprises 34 additional fields:

PGD field	Label	Labelling in PGD	No.	Range	Unit	Type
Mean slope in sector i	$h_{m,i}$	S1D_AVG_SLO_DIRi	8	$0-90$	°	Real
Ratio of slope in sector i	f_i	S1D_FRASP_DIRi	8	$0-1$	–	Real
Mean slope	h	S1D_AVG_SLO	1	$0-90$	°	Real
Sky view factor	δ_{sv}	S1D_AVG_SVF	1	$0-1$	–	Real
Coefficient A_i	A_i	S1D_RSHA_DIRi	8	–	–	Real
Coefficient B_i	B_i	S1D_RSHB_DIRi	8	–	–	Real

4. Tests: New PGD fields

For the calculation of fields in the PGD file was used the digital elevation model (Shuttle Radar Topography Mission SRTM, Rodriguez et al., 2005 with resolution 3-arcseconds (90m in Central Europe). The fields was calculated by external scripts. For tests was used area around the Inn Valley (Innsbruck area) which is reach for the rugged topography. For the

[1]It should be note that, this algorithm is not exactly, see last paragraph.

plots of fields was used fa_api (fa_plot.py tool) by Tomas Kral, Alexandre Mary. We tested all additional fields for all directions.

4.1 Mean slope in sector

On the figure 4.1 are mean slope fields for the representative directions. On the top pannel is plotted the mean slope for the north direction DIR1. First two columns from left are plotted for the PGD files which was written by external scripts. Left is for the resolution 1km and right is for the resolution 2.5km. Third column (for comparism) is plotted for the fields which scripts was written by Méteó France. There are very small differences between them. On the 1km resolution is visible also a more delicate structure. The same results are obtained also for SE, S and NW direction (not shown). On the bottom pannel are ploted for comparism north-east directions. The meaning of the columns is the same. The mean slope calculated by our external is apparently smaller unlike mean slope calculated by Méteó France scripts. The same behaviour is also for E,SW,W (not shown). It is still unknown what is the reason of the differences.

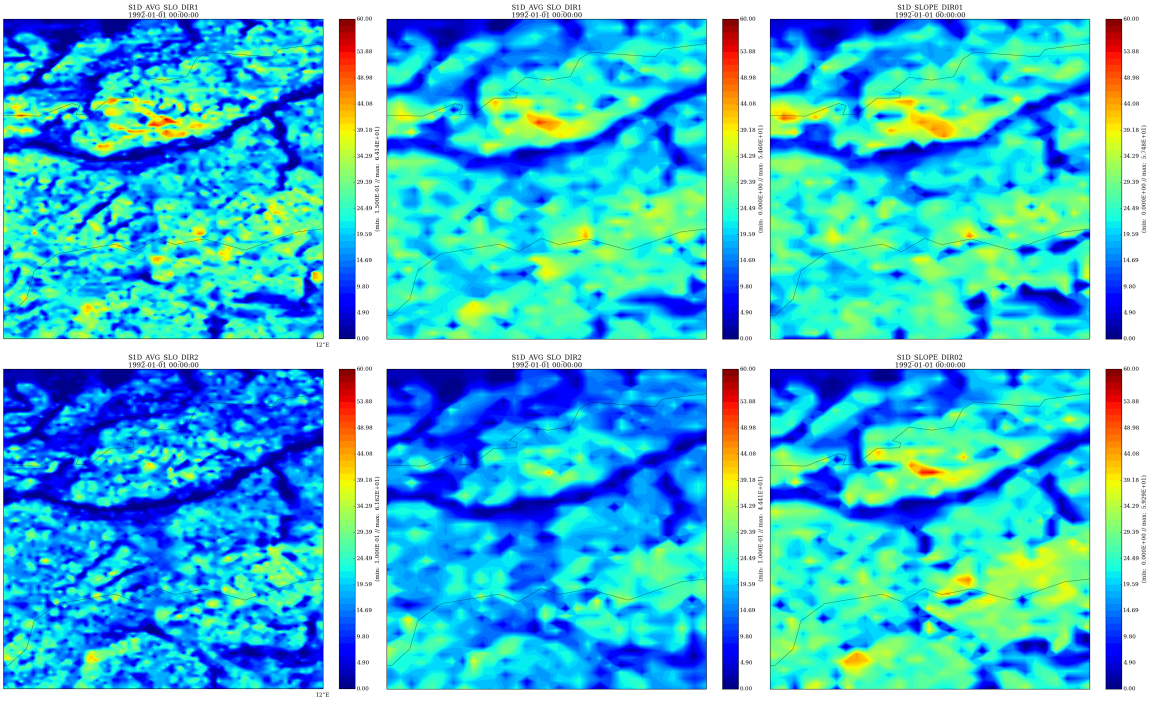

Figure 4.1: Top pannel: Mean slope [degrees] of PGD files in direction N for Innsbruck area. Bottom pannel: Mean slope [degrees] of PGD files in direction NE for Innsbruck area. Left column: External scripts for the model resolution 1km. Middle column: External scripts for the model resolution 2.5km. Right column: Météo-France for the model resolution 2.5km

4.2 Ratio of slope in sectors

On the fig 4.2 is plotted ratio of slope for representative south direction. The meaning of the columns is the same as for previous section (mean slope in sectors). All three figure shows that the maximum amout of slopes oriented to south are situated north from Inn valley,

that is expected. With increasing resolution grows contribution from smaller hills (left figure). The contribution for south slopes calculated by Méteó France is smaller (right image). For annother directions there are also small differences (not shown).

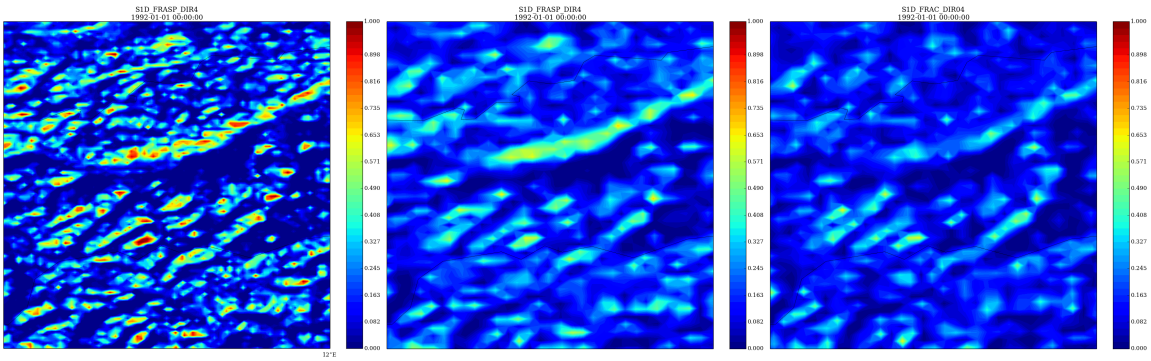

Figure 4.2: Ratio of slope for PGD files in south direction for Innsbruck area. Left column: External scripts for the model resolution 1km. Middle column: External scripts for the model resolution 2.5km. Right column: Météo-France for the model resolution 2.5km

4.3 Mean slope

For control purposes was calculated also average mean slope. Our data are consistent with Météo-France see fig. 4.3.

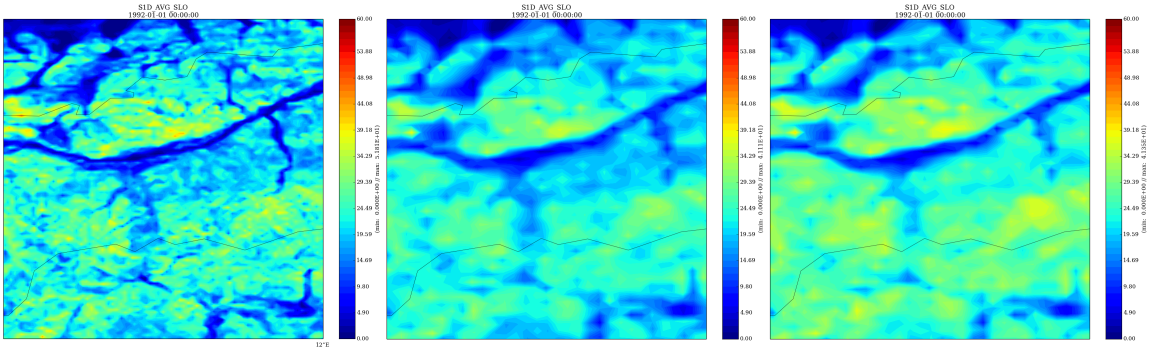

Figure 4.3: Average slope [degrees] of PGD files for Innsbruck area. Left column: External scripts for the model resolution 1km. Middle column: External scripts for the model resolution 2.5km. Right column: Météo-France for the model resolution 2.5km

4.4 Sky view factor

The one of most important field is sky view factor. On the fig. 4.4 are plotted sky view factors for our scripts for resolution 2.5km (top left), for resolution 1km (bottom left), Météo-France for resolution 2.5km (top right) and difference between Météo-France and external scripts for the model resolution 2.5km (bottom right). Our data are qualitative same as Météo-France, but near tops of hills is significantly slower up to 20 %. The difference may be caused that Météo-France calculated the sky view factor only from model resolution i.e. 2.5km, but we calculated the sky view factor from subgrid model SRTM i.e. approx 90m. At

the higher resolution, see 4.4 (bottom left) is visible that in the bottom valeys is the sky view factor smaller.

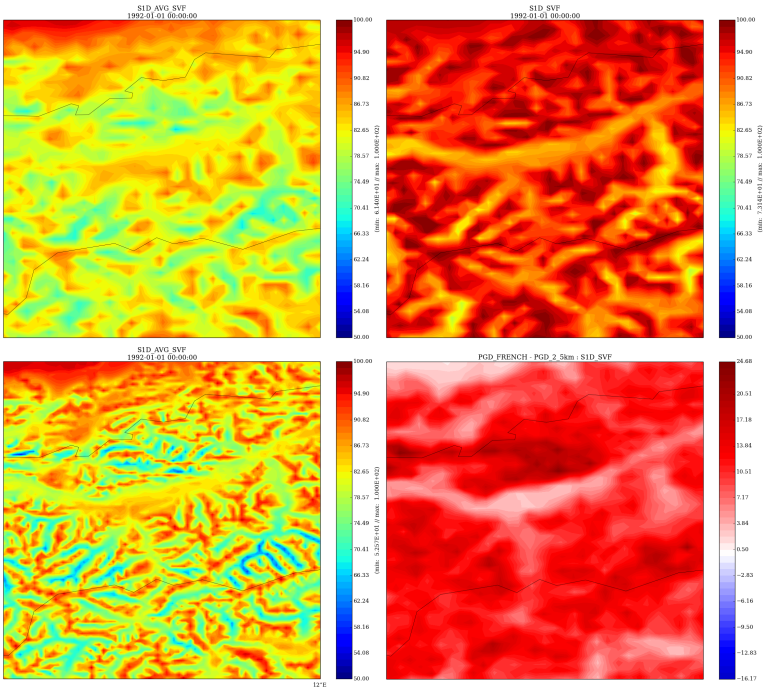

Figure 4.4: Sky view factor [%] of PGD files for Innsbruck area. Top left: External scripts for the model resolution 2.5km. Bottom left: External scripts for the model resolution 1km. Top right: Météo-France for the model resolution 2.5km. Bottom right: Difference between Météo-France and external scripts for the model resolution 2.5km.

4.5 Minimum and maximum local horizons in sector

The plots of A_i and B_i are difficult to understand instead of them, figures of minimum and maximum local horizons in sectors has been plotted, see fig. 4.5 and fig. 4.6. On the fig. 4.5 and 4.6 are plotted minimum (maximum) local horizons in north direction. The minimum local horizon figures are very similar with Metéo-France, but the maximum local horizon is much bigger. Difference between the French minimum and maximum is very small, see right column and it seems to be bad.

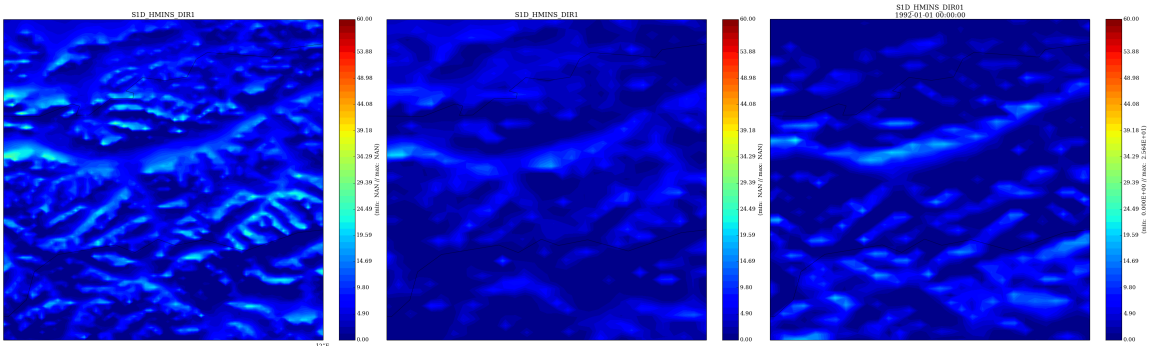

Figure 4.5: Minimum local horizon [degrees] of PGD files in north direction for Innsbruck area. Left column: External scripts for the model resolution 1km. Middle column: External scripts for the model resolution 2.5km. Right column: Météo-France for the model resolution 2.5km

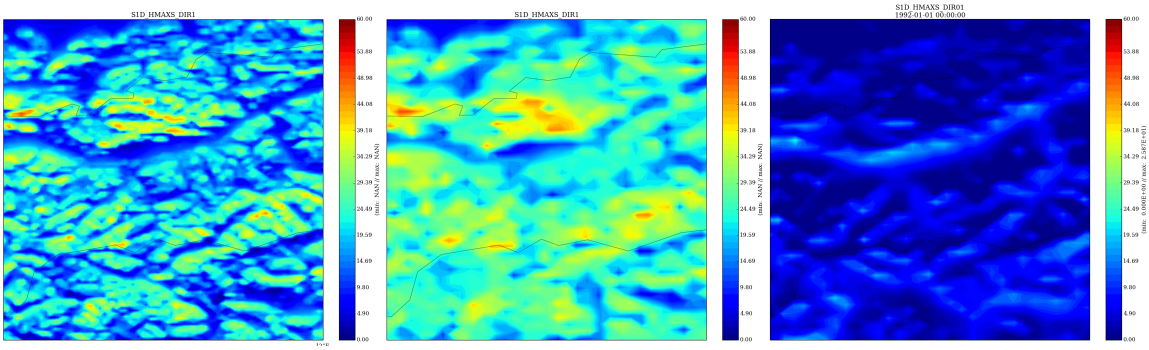

Figure 4.6: Maximum local horizon [degrees] of PGD files in north direction for Innsbruck area. Left column: External scripts for the model resolution 1km. Middle column: External scripts for the model resolution 2.5km. Right column: Météo-France for the model resolution 2.5km

5. Tests: Forecast of observables

The new orographic parametrization has the main influence for forecasts of the global radiation and 2m temperature. We have comperad stations from TAWES databes where we restricted only for stations which the real station sky view factor is less than 80%. For the test was used model run from 12th march 2014 from 00 UTC for 24 hours. During this day was in Austria sunny weather. Global radiation and temperature in 2m was tested. For getting data from AROME was used tool fa_point.py and for plotting GNUPLOT.

5.1 Global radiation

On the fig. 5.1 is plotted time dependet global radiation for St. Leonhard Pitzal. This station has the smallest real sky view factor from TAWES stations (only 69%) . The biggest difference between TAWES global radiation and AROME model without parametrization is in the morning and evening, when the Sun is below local horizon and there is only diffuse global

radiation. When shadowing is switched on, the forecast is better. Also increasing the model resolution has better effect. The sky view restriction a little increase values, that it is propably bad, because mountain obstacles decrease the diffuse solar radiation.

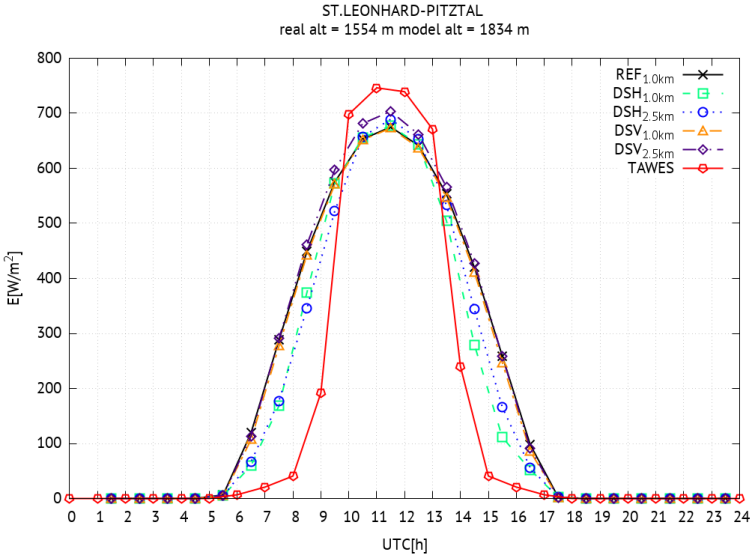

Figure 5.1: Global radiation for St. Leonhard Pitzal. Real station sky view is 69%. The real altitude is 1554 m.a.s.l. The 2.5km model altitude is 2238 m.a.s.l. The 1km model altitude is 1834 m.a.s.l. Red line: TAWES data. Black line: AROME model 1km resolution without orographic parametrization. Green dashed line: 1km resolution with shadowing only. Blue dotted line: 2.5km resolution with shadowing only. Orange dotted-dashed line: 1km resolution with sky view factor only. Purple double dotted-dashed line: 2.5km resolution sky view factor only..

5.2 Temperature in 2m

Comparing temperature plots is little tricky. The main problem is the different elevations of the stations represented in the model AROME and the real elevations of the TAWES stations. The difference may be considerable (a few hundred meters). So the temperature deviations maybe also a few deegres.

For the sample was choosen the station Brennerneu, see. fig. 5.2 where the differences between altitudes are not so high. The shadow effect (DSH) has good influence in the morning and evening(about 0.5 degree correction in 2.5km AROME and 1 degre correction in 1km AROME). The slope correction (DSL) has for this station netrual effect. The sky view restriction (DSV) increase temperature mainly at night. In this case is bad because the the model temperature without new parametrization is higher about 3 deegres than TAWES so error is increasing. For the other stations (not shown in this report) is the behaviour same.

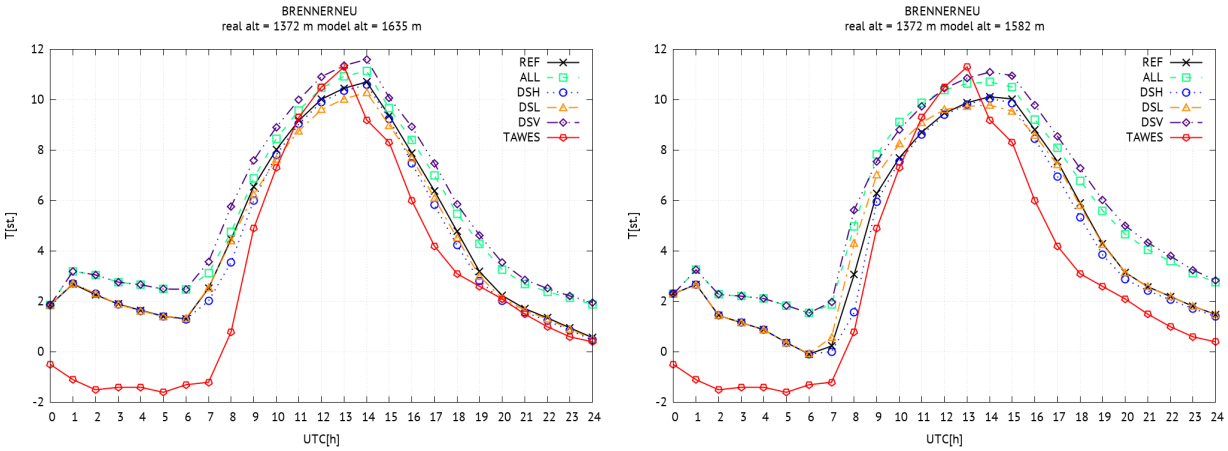

Figure 5.2: Comparison of temperature in 2m in AROME model (2.5km left image, 1km right image)with TAWES for Brennerneu. Real station sky view is 76%. The real altitude is 1372 m.a.s.l. The 2.5km model altitude is 1635 m.a.s.l. . The 1km model altitude is 1582 m.a.s.l. Red line: TAWES data. Black line: AROME model without orographic parametrization. Green dashed line: shadow correction, slope correction and sky view restriction together, Blue dotted line: Shadowing only. Orange dotted-dashed line: slope correction only. Purple double dotted-dashed line: sky view restriction only.

6. Conslusions

We were studying the new parametrization of orography of the model AROME. This physics require 34 additional parametrization fields in the PGD file. We have tested these fields in the area of river Inn, which is very interesting for rugged orography. We have compared PGD fields calculating by external scripts in ZAMG and PGD files caclulating in Metéo-France. In this report was shown, that the new fields in PGD file are in qualitative agreement except local horizon and sky view factor. At first sight it seems that this difference is apparently caused by that French used for these fields only model orography instead of subgrid-scale resolution and therefore are suppressed extrems near mountains. This striking difference but may be caused by an systematic error of calculating of sky view factor. In the script, we have found a bug in weightning local horizon (not shown in this report). We repaired this, but there is may be more delicate bug and therefore it would be appropriate to investigate a more detailed calculation of this field.

We have investigated also dynamics of this model. The most important quantities are time dependent global radiation and 2m temperature. We have comperad the stations data from TAWES databes where we restricted only for stations which the real station sky view factor is less than 80%. For the test was used model run when was in Austria sunny weather. The biggest influence for the global radiation has correction to local horizon (shadowing). This influence is most significantly near sunrise and sunset time when the Sun is below the local horizon. This is in good agreement with stations data. The similar good results for the shadowing are obtained aslo for 2m temperature. The slope effect is depending on the station, for some stations is correction better, for some worse. The worst result is the influence of the sky view factor for the temperature, thats the reason is mentioned in previous paragraph or the model has a general problem with the changed longwave radiation.

In the future may be good more detailed study, i. e. compare calculation of the global radiations and 2m temperature from more runs from different days.

When I was finishing this report, we have talked with Nora Hellbig (radiation expert from Switzerland) that the formula for the calculation of the sky view factor is wrong in our implementation. We used the same formula as in works [3], [4]. In the work Manners et al. [6] say that the formula for the sky view factor is not good. The problem is that we calculated the sky view factor from a horizontal grid point, but in fact we have to consider the slope of the grid cell as well.

Bibliography

[1] C. D. Whiteman, K. J. Allwine, L. J. Fritschen, M. M. Orgill, and J. R. Simpson, J. Appl. Meteor., **28**, 414 (1989).

[2] M. N. Matzinger, M. Andretta, E. Van Gorsel, R. Vogt, A. Ohmura, and M. W. Rotach,Quarr. J. Roy. Meteor. Soc., **129**, 877 (2003).

[3] M. D. Müller, and D. Scherer, American Meteor. Soc., **133**, 1431 (2005).

[4] A. V. Senkova, L. Rontu, and H. Savijärvi, Tellus, **59A**, 279 (2007).

[5] K. Ya. Kondratyev, and M. P. Fedorova, *Radiation regime of inclined surfaces*, WMO, (1977).

[6] J. Manners, S. B. Vosper and N. Roberts, Quarterly Journal of the Royal Meteorological Society, **138**, 720 (2012).